Carbon-based resistive memories

W. W. Koelmans[1]*, T. Bachmann[2†], F. Zipoli[1], A. K. Ott[3], C. Dou[3], A. C. Ferrari[3], O. Cojocaru-Mirédin[4,5], S. Zhang[5], C. Scheu[5], M. Wuttig[4], V. K. Nagareddy[2], M. F. Craciun[2], A. M. Alexeev[2], C. D. Wright[2], V. P. Jonnalagadda[1], A. Curioni[1], A. Sebastian[1], E. Eleftheriou[1]

[1]IBM Research - Zurich, Säumerstrasse 4, 8803 Rüschlikon, Switzerland
[2]College of Engineering, Mathematics and Physical Sciences, University of Exeter, Exeter EX4 4QF, United Kingdom
[3]Cambridge Graphene Centre, University of Cambridge, Cambridge, CB3 0FA, United Kingdom
[4]Institute of Physics (IA), RWTH Aachen University, 52056 Aachen, Germany
[5]Max-Planck Institut für Eisenforschung GmbH, Max-Planck Straße 1, 40237 Düsseldorf, Germany
*wko@zurich.ibm.com, †tb352@exeter.ac.uk

***Abstract*—Carbon-based nonvolatile resistive memories are an emerging technology. Switching endurance remains a challenge in carbon memories based on tetrahedral amorphous carbon (ta-C). One way to counter this is by oxygenation to increase the repeatability of reversible switching. Here, we overview the current status of carbon memories. We then present a comparative study of oxygen-free and oxygenated carbon-based memory devices, combining experiments and molecular dynamics (MD) simulations.**

***Index Terms*—Nonvolatile memory, oxygenated carbon, RRAM, tetrahedral amorphous carbon, diamond-like carbon, storage class memory**

I. Introduction

Resistive random-access memories (RRAM) are heavily researched, because of the significant speed and power benefits they bring to conventional computing architectures [1]. In addition, resistive memory cells have the potential to serve as building blocks in emerging brain-inspired computing and in memcomputing architectures [2]. Amorphous carbon-based resistive memories are gaining traction, as shown by their recent addition (2014) to the selection of emerging memory technologies assessed by the Emerging Research Devices chapter of the International Technology Roadmap for Semiconductors (ITRS) [3].

Amorphous and diamond-like carbons are attractive memory materials. They can be easily manufactured and have a low cost. These materials can change resistance upon the application of unipolar electrical pulses without the need for additional elements [4-8]. Joule heating is thought to be responsible for the structural modifications that bring about the change in resistance [4-6]. The single-elemental nature of carbon enables scaling of memory devices down to very small dimensions, currently down to 50 nm [7]. Smaller devices lead to very low power consumption. The atomic scale changes sufficient to give a resistance variation also give promise for high operating speeds [5]. Moreover, the high resilience of amorphous and diamond-like carbon to a variety of external stimuli, such as heat, friction, wear and corrosion [9,10], also ensures robustness.

Despite the promising potential, carbon memory technology is still at the nascent stage, and a thorough understanding of the resistance changing mechanism is lacking. Nanometer-sized active areas in conjunction with nanosecond switching times create a challenging experimental environment.

Here, we investigate carbon memories through a combination of experimental studies and molecular dynamics (MD) simulations. First, we present MD simulations aimed at understanding the switching mechanism in memory devices based on tetrahedral amorphous carbon (ta-C). Switching endurance, i.e. the number of SET and RESET cycles that can be applied, remains a key challenge for ta-C based memories. One way to counter this is by oxygenation [12]. We present a comparative study of oxygen-free and oxygenated carbon-based memory devices aimed at comparing their performance and find that oxygenated amorphous carbon (a-CO_x) shows better switching endurance, but it comes at the expense of bipolar operation and the need to deviate from single elemental memory devices.

II. Switching Mechanism

Within amorphous or diamond-like carbon, the presence of sp^2 chains can lead to an electrically conductive state, when conjugated, whereas sp^3-dominated carbon yields a high resistance. The two known mechanisms by which amorphous carbon switches from high to low resistance, are re-hybridizing carbon atoms from sp^3 to sp^2 [4] and arranging the sp^2 hybridized atoms so that they form a conductive pathway [5].

We perform atomistic simulations to study the resistance switching mechanisms in ta-C based on an augmented-Tersoff classical potential for large scale molecular-dynamics simulations lasting tens of ns for systems containing up to two million atoms using box sizes up to 27 × 27 × 18 nm^3, see Fig. 1. We also use density-functional theory on smaller systems to link the structural and electronic properties.

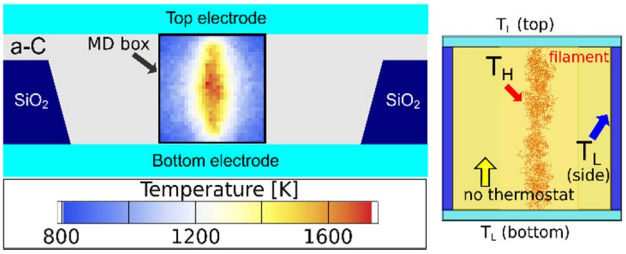

Fig. 1. Schematic depiction of the amorphous carbon memory cell. Also indicated is the box that is simulated by the MD simulations.

978-1-4673-8833-7/16/$31.00 ©2016 IEEE

In our classical simulations we model the heat produced by the passage of an electric current using multiple thermostats, see the inset of Fig. 1. Our model assumes that the main effect of the electric field is to heat the system via an increase of temperature (T) of the atoms forming conducting pathways between the electrodes. The amount of Joule heat is higher where the current is higher, i.e., along the pathways with a higher density of sp^2 atoms. The simulation results heavily depend on the box boundary conditions: constant pressure, which allows expansion, or constant volume, which does not. This dependency is caused by the strong link between the sp^3 content and the atomic density. Assuming that overall the ta-C density cannot change significantly, we then use a constant volume approach. We consider different sp^3 contents between 40 % and 80 % and densities between ~ 2.6 g/cm^3 and ~ 3 g/cm^3.

We simulate the SET steps by enforcing a high temperature T_H = 1500 K to the atoms in this conductive region via a thermostat. We simulate the RESET step by heating between 1500 and 2500 K, see Fig. 2, where T_H ~ 2500 K would correspond to an aggressive RESET. For both SET and RESET, two additional thermostats, set to a low temperature, T_L = 300-500 K, are coupled to the atoms located in the blue and cyan regions in the inset of Fig. 1 to take into account the heat dissipated via the electrodes and the surrounding a-C matrix.

No SET occurs below 1500 K. For $T \geq$ 1500K a continuous, conductive filament is formed. Note that these T are in part overestimated because our model neglects the weakening of the covalent bonds due to the passage of current, which can lower the bond breaking barrier.

During SET, part, e.g., 2-3 %, of the sp^3 atoms in the T_H region re-hybridizes to sp^2. The a-C matrix in the vicinity of the T_H-region accommodates the related expansion by increasing its density from ~ 2.4 g/cm^3 to ~ 3 g/cm^3, when going from the filament to ~ 20 Å away from it, via the reverse re-hybridization of sp^2 to sp^3. Over the entire box, we observe marginal changes of the sp^3 content, below 1-2 %. For sp^3 > 35 %, the maximum size of sp^2 clusters is limited to fewer than a thousand atoms. If sp^3 < 35 %, an irreversible extended sp^2 domain percolating through the entire system is formed during SET.

During RESET, a few hundred atoms, among the few thousand that form the conductive pathway shown in Fig. 2, are re-hybridized from sp^2 to sp^3. This re-hybridization fragments the filament into smaller sp^2 clusters.

A key insight from the MD simulations is the role played by the T gradients in reversible switching. The more efficiently heat is dissipated in the direction orthogonal to the filament, the more confined is the region that undergoes re-hybridization. In particular, dissipation of heat through the surrounding matrix helps the SET process by inducing the formation of elongated clusters that eventually merge into a single conjugated filament percolating from the top to the bottom electrodes. Heat dissipation from the top and the bottom electrodes, in the direction of the filament, helps the RESET step. Reversible switching does not occur without T gradients, thus a-C differs from phase-change materials, which can be molten and rapidly quenched in the high resistance amorphous state [11] or slowly quenched in the low resistance crystalline phase [11]. In a-C, sp^2 clusters are stable, they form after a couple of ns and, when heated uniformly, these clusters do not break up easily.

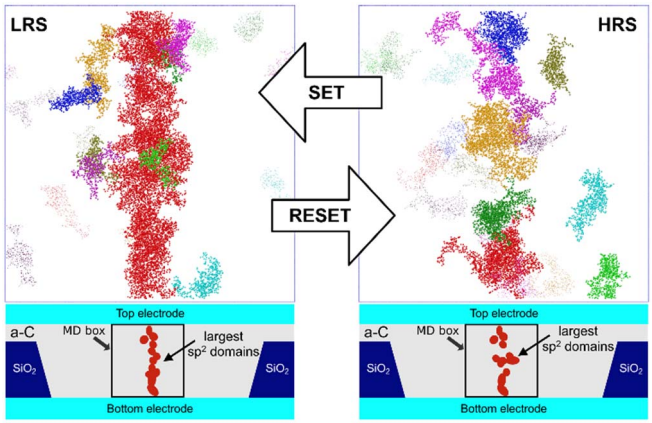

Fig. 2. MD simulation result of filamentary switching in t-aC for low resistance (LRS) and high resistance state(HRS). For the SET and RESET states, sp^2 carbon atoms are shown. Each color represents a different cluster of conjugated sp^2 atoms.

The requirements on sp^3 content, e.g., it should not be < 35 %, and T gradients make repeatable reversible switching a key challenge in ta-C-based memories. One way to counter this is by the oxygenation of carbon. Oxygenation assists the RESET process by introducing an electrochemical component to the switching mechanism [12]. In the pristine state, electrical transport is dominated by the bulk material that is in a high-resistance state. There is also a strong field dependence of the resistivity and at ~ 3 V between top- and bottom electrode, a dielectric breakdown or threshold-switching behavior occurs: a few hundred μA current flows through the device, which goes into a low-resistance SET state. Here, transport is dominated by conductive filaments predominantly consisting of reduced a-CO_x. Due to oxygen-ion migration towards the bottom electrode, these filaments behave similar to filaments in ta-C, therefore they may predominantly consist of graphitic clusters of sp^2 carbon atoms. A RESET state of higher resistance is recovered by application of the RESET pulse. A partial rupture of the conductive filaments occurs, assisted by the release of oxygen ions trapped in the bottom electrode [12]. Oxygenation is thus a promising approach, even though this comes at the cost of bipolar operation, where the SET operation takes place on one polarity of the voltage, and the RESET operation requires the opposite polarity, as well as the need to incorporate an additional element into the memory material.

III. Memory Devices

Memory devices, schematically depicted in Fig. 1, are fabricated on Si wafers with thermally grown SiO_2. They consist of a bottom electrode of sputtered Pt with a layer of sputtered SiO_2 on top. Openings of 50 to 200 nm diameter are etched into the SiO_2, and either ta-C or a-CO_x is deposited into them to form individual memory cells of various sizes. The top electrode is sputtered W. The ta-C films are deposited by a single bend filtered cathodic vacuum arc (FCVA) [13]. During deposition, the arc is struck only once per chip to avoid the formation of a multi-layer ta-C stack within the memory cells that could

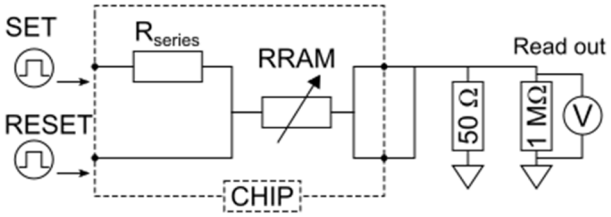

Fig. 3. High-speed electrical circuitry showing the chip with series resistor and RRAM cell. Pulses are generated off-chip by a generator and the current is read using an oscilloscope with 1 MΩ termination. Relays (not shown) are used to switch between SET and RESET operations.

influence the resistive switching behavior. Using multi-wavelength Raman characterization [14-16] we determine the G peak dispersion, e.g., the change in G peak position with wavelength, and extract the bonding parameters such as the Young's modulus, the density and the sp^3 content. The ta-C films have ~ 50% sp^3 bonds

The a-CO_x is deposited by DC magnetron physical vapor deposition with a graphitic carbon target and a 15 % O_2/Ar gas mixture. Raman characterization shows that oxygen breaks the sp^2 rings, which predominate in sputtered carbon [12].

After fabrication, each cell can be accessed via two sets of pads, see Fig. 3. In the absence of a transistor, access via one set of pads adds a built-in series resistor to the electrical path to limit the current during SET operation. The built-in series resistor is defined by e-beam lithography to keep its surface area small and the parasitic capacitance low. The RESET operation uses the path without an explicit series resistor.

A cell of 75 nm in diameter filled with 20 nm ta-C is programmed in the SET state and inspected using a high-angle annular dark field (HAADF) scanning transmission electron microscopy (STEM). The encapsulation of SiO_2 was etched away as well as (part of) the tungsten top electrode, see Fig. 4. The images show that, even after bringing the cell to the SET state, no intermixing of elements has taken place.

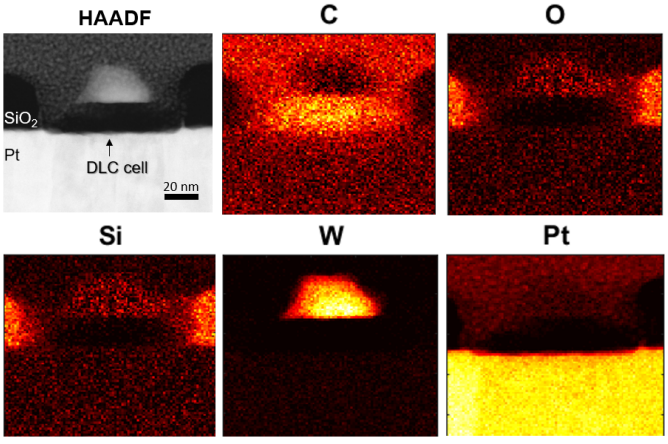

Fig. 4. HAADF STEM image of a ta-C memory cell in the SET state and EDS spectral images from the same cell showing the redistribution of various elements. The ta-C has a high purity and no tungsten or platinum is found inside the cell.

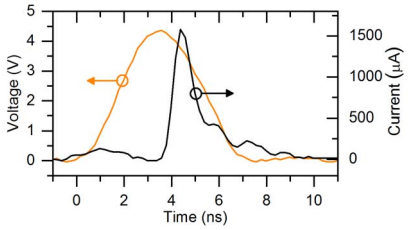

Fig. 5. A ta-C forming pulse with a duration of 4 ns.

IV. Performance Characterization

A. Tetrahedral amorphous carbon

Initially, the ta-C memory cell, with a layer of 5 nm ta-C, is in a high resistive state. Applying a forming pulse, see Fig. 5, the cell is brought to a low resistance state with the current-limiting resistor (3-14 kΩ) in series. The forming pulse is very fast, ~ 4 ns, but it has a higher voltage and peak current than a typical SET operation, Fig. 6b. A typical SET pulse is less than 60 ns and the switching itself occurs within several ns. Note that the spike in the current, observed at 30 ns, corresponds to the point at which the cell switches and that the spike height is determined by parasitic capacitance discharge. The RESET pulse has to be faster than the SET to prevent the cell from setting again after resetting (during the same RESET pulse).

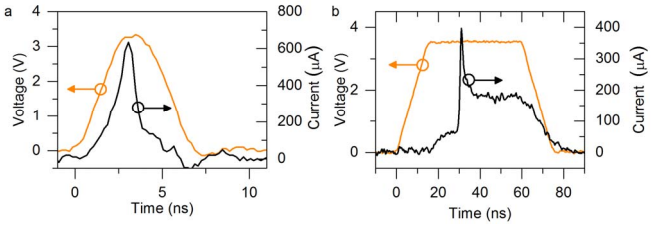

Fig. 6. a) Typical high-speed RESET pulse for ta-C of ~ 4 ns and b) typical high-speed SET pulse of ~ 50 ns. After the maximum SET voltage is reached it takes less than 15 ns for the cell to react and it then switches to the low resistance state within 2 ns.

In Fig. 6a, a typical 4-ns-long RESET pulse is shown. The switching takes places in 2 ns. The RESET is performed without the resistor in series, hence a higher current is reached.

The switching is repeatable as shown in Fig. 7, in which more than 100 cycles are shown. As predicted by the MD simulations, better control of the sp^3 content and T gradients might lead to higher endurance. However, achieving more than several hundred cycles remains a challenge.

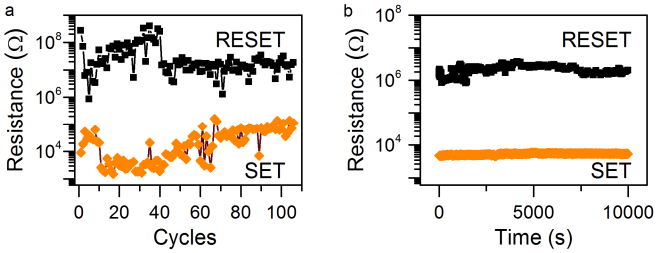

Fig.7. a) Memory endurance of ta-C tested to be more than 100 cycles b) Retention measurements of SET and RESET states at 85°C. All resistances were measured at a bias voltage of 0.2 V.

B. Oxygenated carbon

a-CO_x-based memory devices are initially in a very high-resistance state and need a forming pulse typically 2 µs long [12]. Unlike ta-C-based memory devices, they need to be operated in a bipolar fashion. Here we show ultra-fast RESET pulses of 4 ns duration, see Fig. 8a, and also the fastest SET pulses reported on a-CO_x to date, see Fig. 8b. The devices have 18-nm-thick a-CO_x.

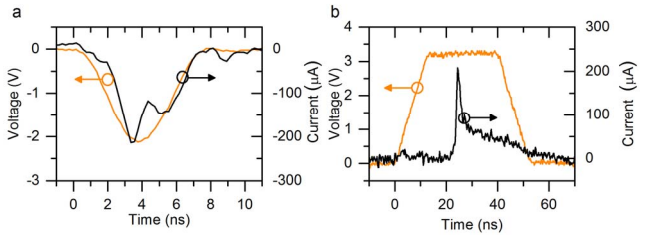

Fig. 8. a) Typical high-speed RESET pulse for a-CO_x of ~ 4 ns and b) typical high-speed SET pulse of ~ 40 ns. After the maximum SET voltage has been reached it takes less than 12 ns for the cell to react and it then switches to the low resistance state within 2 ns.

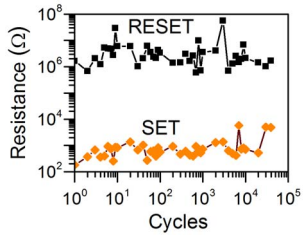

Fig. 9. Memory endurance of a-CO_x tested to over 10^4 cycles. From [12].

The endurance of a-CO_x [12] is compared in Fig. 9 with that of ta-C. The larger endurance of 10^4 cycles is attributed to the presence of oxygen, which significantly assists the RESET.

C. Comparison

In Table 1 we summarize the main specifications for the ta-C and a-CO_x samples studied here.

TABLE 1. COMPARISON OF OUR TA-C AND A-CO_x-BASED MEMORY DEVICES

	ta-C		**a-CO_x**	
	SET	**RESET**	**SET**	**RESET**
Pulse duration	50 ns*	4 ns*	40 ns*	4 ns*
Switch energy	15 pJ*	3 pJ*	2 pJ*	1 pJ*
Forming	4 ns @ 2 pJ*		2 µs [12]	
Endurance	> 100*		40,000 [12]	
Retention	10,000 s @ 85°C*		10,000 s @ 85°C [12]	

* This work

V. CONCLUSIONS

We investigated carbon-based resistive memory devices based on ta-C and a-CO_x. We explored the switching mechanism in ta-C-based memory devices via MD simulations. We found that reversible switching requires a minimum of 35 % sp^3. We also discussed the role of heat dissipation and temperature gradients. Lateral heat dissipation aids the SET operation, whereas vertical heat dissipation through the top and bottom electrodes aided the RESET operation. Oxygenation of carbon serves as a promising alternative even though it comes at the cost of bipolar operation and the need to deviate from a single elemental memory material. Oxygenation assists the RESET process by introducing an electrochemical component to the switching mechanism. We designed and fabricated ta-C and a-CO_x-based memory devices and tested them. ta-C switches in both unipolar and bipolar manner, whereas a-CO_x is best operated in bipolar manner. High speed (< 50 ns) switching was demonstrated for both memory types. Switching energies are remarkably low, ranging from 1 to 15 pJ. The significant difference is in terms of the switching endurance, where a-CO_x is better than the ta-C samples used here. We believe that the insights gained from our simulations and experiments will further progress this promising memory technology.

ACKNOWLEDGMENT

We thank C. Santini for early contributions to this work. This work is funded by the EU research & innovation project CareRAMM, no. 309980.

VI. REFERENCES

[1] H.-S. P. Wong, S. Salahuddin, Nat. Nano. **10**, 191 (2015).
[2] M. Di Ventra and Y. Pershin, Nat. Phys. **9**, 200 (2013).
[3] http://www.itrs2.net/itrs-reports.html
[4] F. Kreupl *et al.*, IEEE International Electron Devices Meeting pp. 1–4 (2008).
[5] A. Sebastian *et al.*, New J. Phys. **13**, 013020 (2011).
[6] D. Fu *et al.*, IEEE Electron Device Lett. **32**, 803 (2011).
[7] J. Xu *et al.*, Carbon **75**, 255 (2014).
[8] L. Dellmann *et al.*, in Proc. 43rd European Solid-State Device Research Conf., 2013.
[9] S. R. P. Silva, "Properties of amorphous carbon", INSPEC, The Institution of Electrical Engineers, London, 2003.
[10] A. C. Ferrari *et al.*, J. Appl. Phys. **85**, 7191 (1999).
[11] S. Raoux *et al.* MRS Bulletin **39**, 703 (2014).
[12] C. A. Santini *et al.*, Nat. Comm. **6**, 8600 (2015).
[13] M. C. Polo *et al.,* Diam. Rel. Mater. **9**, 663 (2000).
[14] A. C. Ferrari and J. Robertson, Phys. Rev. B **61**, 14095 (2000).
[15] A. C. Ferrari and J. Robertson, Phys. Rev. B **64**, 075414 (2001).
[16] A. C. Ferrari, Surf. Coat. Technol. **180-181**, 190 (2004).